



Year: 2023

Generation of a novel fully human non-superagonistic anti-CD28 antibody with efficient and safe T-cell co-stimulation properties

Elsayed, Abdullah ; Pellegrino, Christian ; Plüss, Louis ; Peisert, Frederik ; Benz, Ramon ; Ulrich, Franziska ; Thorhallsdottir, Gudrun ; Plaza, Sheila Dakhel ; Villa, Alessandra ; Mock, Jacqueline ; Puca, Emanuele ; De Luca, Roberto ; Manz, Markus G ; Halin, Cornelia ; Neri, Dario

Abstract: Antibody-based therapeutics represent an important class of biopharmaceuticals in cancer immunotherapy. CD3 bispecific T-cell engagers activate cytotoxic T-cells and have shown remarkable clinical outcomes against several hematological malignancies. The absence of a costimulatory signal through CD28 typically leads to insufficient T-cell activation and early exhaustion. The combination of CD3 and CD28 targeting products offers an attractive strategy to boost T-cell activity. However, the development of CD28-targeting therapies ceased after TeGenero's Phase 1 trial in 2006 evaluating a superagonistic anti-CD28 antibody (TGN1412) resulted in severe life-threatening side effects. Here, we describe the generation of a novel fully human anti-CD28 antibody termed "E1P2" using phage display technology. E1P2 bound to human and mouse CD28 as shown by flow cytometry on primary human and mouse T-cells. Epitope mapping revealed a conformational binding epitope for E1P2 close to the apex of CD28, similar to its natural ligand and unlike the lateral epitope of TGN1412. E1P2, in contrast to TGN1412, showed no signs of *in vitro* superagonistic properties on human peripheral blood mononuclear cells (PBMCs) using different healthy donors. Importantly, an *in vivo* safety study in humanized NSG mice using E1P2, in direct comparison and contrast to TGN1412, did not cause cytokine release syndrome. In an *in vitro* activity assay using human PBMCs, the combination of E1P2 with CD3 bispecific antibodies enhanced tumor cell killing and T-cell proliferation. Collectively, these data demonstrate the therapeutic potential of E1P2 to improve the activity of T-cell receptor/CD3 activating constructs in targeted immunotherapeutic approaches against cancer or infectious diseases.

DOI: <https://doi.org/10.1080/19420862.2023.2220839>

Posted at the Zurich Open Repository and Archive, University of Zurich

ZORA URL: <https://doi.org/10.5167/uzh-239007>

Journal Article

Published Version



The following work is licensed under a Creative Commons: Attribution-NonCommercial 4.0 International (CC BY-NC 4.0) License.

Originally published at:

Elsayed, Abdullah; Pellegrino, Christian; Plüss, Louis; Peisert, Frederik; Benz, Ramon; Ulrich, Franziska; Thorhallsdottir, Gudrun; Plaza, Sheila Dakhel; Villa, Alessandra; Mock, Jacqueline; Puca, Emanuele; De Luca, Roberto;

Manz, Markus G; Halin, Cornelia; Neri, Dario (2023). Generation of a novel fully human non-superagonistic anti-CD28 antibody with efficient and safe T-cell co-stimulation properties. *mAbs*, 15(1):2220839.
DOI: <https://doi.org/10.1080/19420862.2023.2220839>

REPORT



Generation of a novel fully human non-superagonistic anti-CD28 antibody with efficient and safe T-cell co-stimulation properties

Abdullah Elsayed^{a,b}, Christian Pellegrino^c, Louis Plüss^{a,b}, Frederik Peisert^a, Ramon Benz^b, Franziska Ulrich^b, Gudrun Thorhallsdottir^{a,b}, Sheila Dakhel Plaza^a, Alessandra Villa^a, Jacqueline Mock^a, Emanuele Puca^a, Roberto De Luca^a, Markus G. Manz^c, Cornelia Halin^b, and Dario Neri^{a,b,d}

^aPhilochem AG, Libernstrasse 3, Otelfingen, Switzerland; ^bDepartment of Chemistry and Applied Biosciences, Swiss Federal Institute of Technology (ETH Zürich), Zurich, Switzerland; ^cDepartment of Medical Oncology and Hematology, University Hospital Zurich and University of Zurich, Zurich, Switzerland; ^dPhiloGen SpA, Siena (S), Italy

ABSTRACT

Antibody-based therapeutics represent an important class of biopharmaceuticals in cancer immunotherapy. CD3 bispecific T-cell engagers activate cytotoxic T-cells and have shown remarkable clinical outcomes against several hematological malignancies. The absence of a costimulatory signal through CD28 typically leads to insufficient T-cell activation and early exhaustion. The combination of CD3 and CD28 targeting products offers an attractive strategy to boost T-cell activity. However, the development of CD28-targeting therapies ceased after TeGenero's Phase 1 trial in 2006 evaluating a superagonistic anti-CD28 antibody (TGN1412) resulted in severe life-threatening side effects. Here, we describe the generation of a novel fully human anti-CD28 antibody termed "E1P2" using phage display technology. E1P2 bound to human and mouse CD28 as shown by flow cytometry on primary human and mouse T-cells. Epitope mapping revealed a conformational binding epitope for E1P2 close to the apex of CD28, similar to its natural ligand and unlike the lateral epitope of TGN1412. E1P2, in contrast to TGN1412, showed no signs of *in vitro* superagonistic properties on human peripheral blood mononuclear cells (PBMCs) using different healthy donors. Importantly, an *in vivo* safety study in humanized NSG mice using E1P2, in direct comparison and contrast to TGN1412, did not cause cytokine release syndrome. In an *in vitro* activity assay using human PBMCs, the combination of E1P2 with CD3 bispecific antibodies enhanced tumor cell killing and T-cell proliferation. Collectively, these data demonstrate the therapeutic potential of E1P2 to improve the activity of T-cell receptor/CD3 activating constructs in targeted immunotherapeutic approaches against cancer or infectious diseases.

ARTICLE HISTORY

Received 17 February 2023
Revised 20 May 2023
Accepted 30 May 2023

KEYWORDS

bispecific antibodies; cancer immunotherapy; CD28; CD3; monoclonal antibodies; phage display technology; protein engineering; tumor targeting

Introduction

Cytotoxic T cells are key mediators of the adaptive immune system to fight cancer. The discovery of the T-cell receptor (TCR) revealed the mechanism of how T cells become activated upon antigen recognition.^{1–3} TCR engagement is initiated by recognizing antigenic peptides, such as tumor antigens, presented by the major histocompatibility complex (MHC) on antigen-presenting cells (APCs) and tumor cells.^{4,5} TCRs lack an intracellular signaling domain. Therefore, their association with CD3 and other co-receptors (e.g., CD4, CD8) is necessary to trigger an activation signal cascade, referred to as "signal 1."^{6–9} However, signal 1 alone is typically insufficient for the full activation of T cells. The absence of an additional signal induces T-cell anergy and impairs T-cell activity.^{10,11} The CD28 receptor provides a crucial costimulatory signal that enhances T-cell proliferation, survival, and production of key cytokines (e.g., IL-2); this costimulatory effect is referred to as "signal 2."^{12–15} CD28 is a homo-dimeric glycoprotein that is constitutively expressed on the surface membrane of most T cells (around 95% of CD4⁺ and 50% of CD8⁺ T cells).¹⁶ In

the immune synapse, CD28 binds to its counter receptors, CD80 and CD86, primarily expressed on APCs.^{17–21}

In T-cell redirection therapy, the integration of signal 1 (via CD3) and signal 2 (via CD28) has shown remarkable antitumor activity.²² For instance, first-generation chimeric antigen receptor (CAR) T-cell therapy, based on CD3 domains only, suffered from early exhaustion and impaired *in vivo* persistence.^{23–25} The potency was significantly improved after adding costimulatory domains, such as CD28, leading to the Food and Drug Administration's approval of Yescarta® (axicabtagene ciloleucel) in 2017 for the treatment of diffuse large B cell lymphoma.^{26–29} A similar approach was also adapted to enhance the activity of CD3-targeting bispecific T-cell engagers (BiTEs). For example, the combination of an activating anti-CD28 monoclonal antibody (mAb) with an anti-CD33/anti-CD3 BiTE (AMG 330) improved the cytotoxicity against multiple acute myeloid leukemia (AML) cell lines.³⁰ Several CD28-targeting bispecific antibodies, such as REGN5668 (anti-Muc16/anti-CD28), are currently being investigated in clinical trials.^{31,32}

CONTACT Dario Neri  dario.neri@philogen.com  Philochem AG, Libernstrasse 3, Otelfingen 8112, Switzerland

 Supplemental data for this article can be accessed online at <https://doi.org/10.1080/19420862.2023.2220839>

© 2023 Philochem AG. Published with license by Taylor & Francis Group, LLC.

This is an Open Access article distributed under the terms of the Creative Commons Attribution-NonCommercial License (<http://creativecommons.org/licenses/by-nc/4.0/>), which permits unrestricted non-commercial use, distribution, and reproduction in any medium, provided the original work is properly cited. The terms on which this article has been published allow the posting of the Accepted Manuscript in a repository by the author(s) or with their consent.

Despite the crucial role of CD28 in cancer immunotherapy, safety concerns halted development of CD28-targeting therapeutics following the TeGenero incident. In 2006, a first-in-human Phase 1 clinical trial was initiated in which all six volunteers, who received TeGenero's TGN1412 mAb, developed life-threatening side effects, including multiple-organ failures due to cytokine release syndrome (CRS).³³ TGN1412 is a superagonistic mAb that can fully activate T-cells via cross-linking CD28 molecules without signal 1, unlike conventional anti-CD28 mAbs.³⁴ TGN1412 binds a particular epitope (laterally exposed C" D loop) close to the cell surface membrane of T cells.³⁵ By contrast, most conventional anti-CD28 mAbs bind close to the natural binding site of CD80/CD86 (near the MYPPPY loop) at the apical part of the receptor.³⁵ In rat models, anti-CD28 superagonistic mAbs induced the proliferation of T cells without noticeable toxicity.^{34,36} In cynomolgus monkeys, TGN1412 was well tolerated at 5 and 50 mg/kg doses; therefore, a proposed dose of 0.1 mg/kg in humans was considered safe.^{37,38} The failure to predict the toxicity of TGN1412 at a preclinical level was attributed to three main factors. First, TGN1412 did not induce *in vitro* cytokine release when added to human peripheral blood mononucleated cells (PBMCs), unless artificially coated on a solid support.³⁹ Second, it was shown that tissue-resident CD4⁺ effector memory (CD4⁺ EM) cells are the primary source of cytokine release; these cells are rare or absent in young and clean laboratory rats.^{39,40} Third, CD4⁺ EM cells in cynomolgus monkeys down-regulate CD28; thus, the toxicity could not have been predicted based on studies in non-human primates.⁴⁰ However, the TeGenero incident sparked a debate in the scientific community on whether the adverse events, including CRS, should have been predicted based on the available knowledge of the CD28 receptor and the expected pharmacological action of TGN1412.^{41–43} Overall, the TeGenero tragedy highlighted the importance of having a translational preclinical model that can predict the toxicity of any tested biologic. Chunting *et al.* has recently shown that humanized NSG mice engrafted with human PBMCs represent an effective model for predicting CRS induced by TGN1412 and other immunomodulatory agents, such as anti-CD3 mAbs.⁴⁴

Considering the TGN1412 toxicity, new agonistic mAbs against CD28 that better resemble the natural ligands are needed to offer a better safety profile while providing a strong costimulatory signal to unleash the full T-cell activity against cancer. Here, we describe the generation, characterization, and *in vivo* safety validation of a new anti-human CD28 mAb termed "E1P2." E1P2 is a fully human mAb isolated by phage display technology from our AMG synthetic library.⁴⁵ E1P2 binds to human and mouse CD28, facilitating preclinical testing. Unlike TGN1412, E1P2 did not activate human PBMCs *in vitro* without TCR/CD3 stimulation. However, E1P2 showed a strong costimulatory effect when combined with an anti-CD3 mAb (OKT3) or a CD3-targeting BiTE, mimicking the function of the endogenous CD80/CD86. Epitope mapping revealed that E1P2 binds close to the natural CD80/CD86 binding region. A toxicity study in NSG mice showed no signs of CRS from E1P2 compared to TGN1412. Collectively, these data support the development of E1P2 as an immunomodulatory agent for boosting T-cell activity toward

difficult-to-treat tumors or as a modular building block for the construction of immunostimulatory therapeutics.

Results

Isolation of fully human anti-CD28 antibodies by phage display

Phage display technology allows the implementation of antibody discovery strategies that may be biased toward a given epitope within a target protein of interest.⁴⁶ For the execution of antibody phage display selections, we cloned and expressed the extracellular domain (ECD) of human CD28 with an Fc tag for homo-dimerization and an AviTag™ for site-specific biotinylation (the amino acid sequence is highlighted in Supplementary Figure S1). The biotin moiety was attached to the membrane-proximal part of CD28, near the C" D loop (the epitope of most superagonistic antibodies),³⁵ to favor the isolation of binders toward the apex of CD28. The homogeneity of the recombinant protein was confirmed by size exclusion chromatography (SEC) and SDS-PAGE [Supplementary Figure S2A]. Binding to a commercial anti-CD28 mAb was shown by ELISA [Supplementary Figure S2B]. A synthetic phage display single-chain variable fragment (scFv) library (AMG)⁴⁵ was screened against the recombinant human CD28 antigen by an affinity capture procedure [Figure 1A]. After two rounds of panning, 92 random clones were picked and screened by ELISA on the human CD28 Fc fusion protein and in parallel on human IgG₁ to exclude potential binders against the Fc portion [Supplementary Figure S3]. Positive clones were analyzed by sequencing, resulting in seven unique clones. All clones shared a partial consensus in the amino acid sequence of both CDR3 loops, highlighting that the selection favored binders against a distinct epitope. All binders were cloned into an IgG₄ format and expressed in Chinese hamster ovary (CHO) cells. Clone "E1P2" was selected based on purity, stability, expression yield, and binding to T cells by flow cytometry. The purity and homogeneity of IgG₄(E1P2) were evaluated by SEC and SDS-PAGE [Figure 1B].

Binding of E1P2 to human and mouse CD28 by ELISA

ScFv(E1P2) was expressed in *E. coli*, and the affinity to human CD28 was assessed by ELISA, revealing an EC₅₀ value of 31 nM [Supplementary Figure S4]. Similarly, E1P2 and TGN1412 in IgG₄ format were tested by ELISA on human and mouse CD28 to calculate the apparent affinity and to check for cross-reactivity [Supplementary Figure S5]. IgG₄(E1P2) showed binding to both human and mouse CD28 with EC₅₀ values of 2.7 nM and 18.5 nM, respectively. By contrast, TGN1412 only bound human CD28 with an EC₅₀ value of 4.4 nM.

Binding of E1P2 to human and mouse T cells by flow cytometry

Flow cytometry was performed on purified primary human and mouse T cells to confirm the binding of E1P2 to the natural CD28 receptor expressed on T cells. IgG₄(E1P2) and

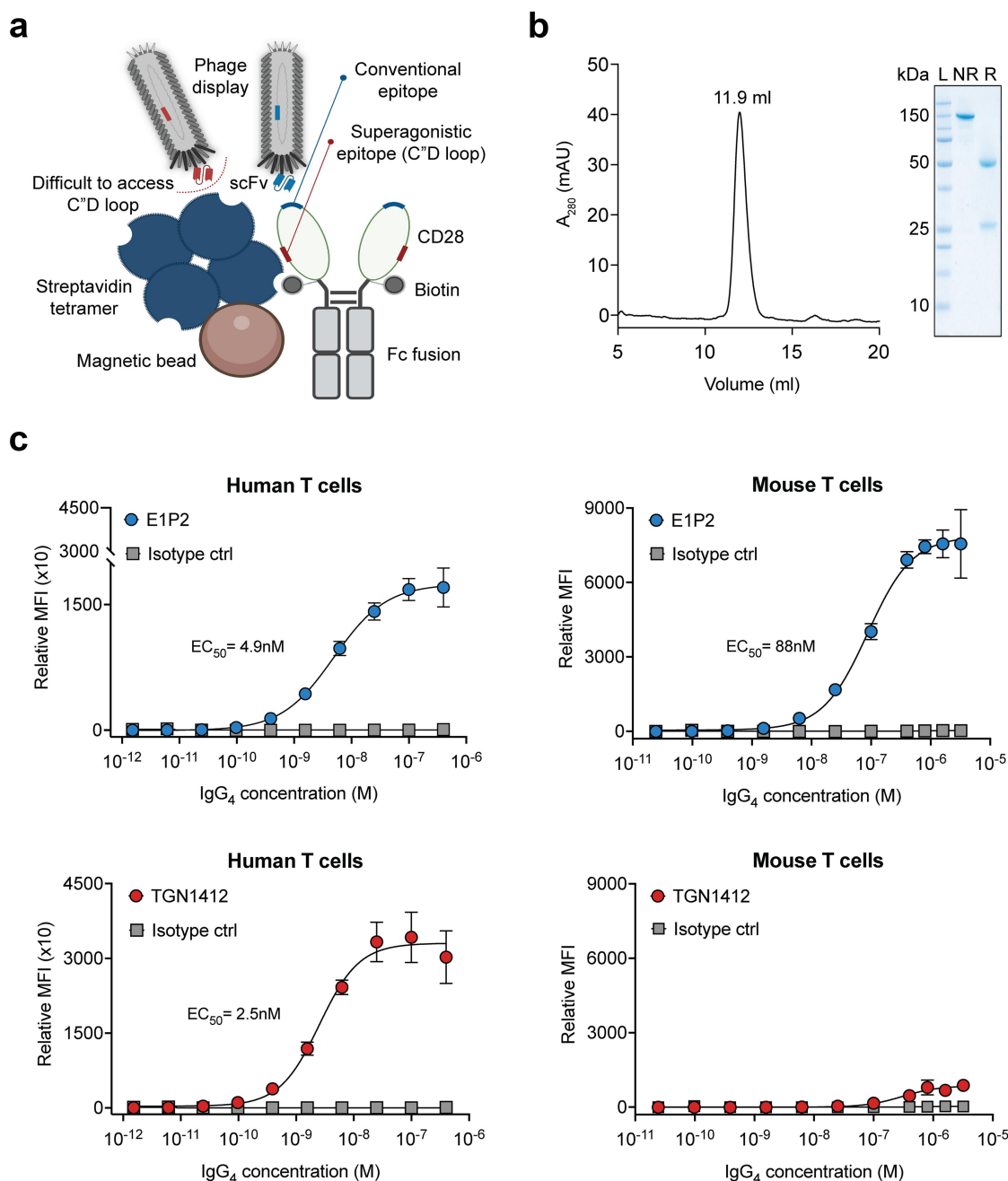


Figure 1. Generation and characterization of E1P2 monoclonal antibody. (a) Schematic representation of the phage display selection strategy to isolate new mAbs toward human CD28. The recombinant human CD28 protein was engineered with a biotin tag close to the superagonistic region (C'D loop), to favor the isolation of binders toward the apex of CD28. (b) IgG₄(E1P2) shows a pure protein with the expected molecular weight in the SEC (left) and SDS-PAGE (right). (c) Binding of IgG₄ (E1P2) and TGN1412 to primary human and mouse T cells by flow cytometry. Only E1P2 bound to both human and mouse T cells (with 18-fold lower apparent affinity to mouse CD28). Data are presented as mean \pm SD of technical triplicates from three independent flow cytometry measurements. MFI was calculated, and the sigmoid curve for antibody concentration (x-axis) against relative MFI (y-axis) was plotted and fitted using a 4-parameter logistic (4PL) non-linear regression model to calculate the EC_{50} values. SEC: size exclusion chromatography; L: ladder; R: reducing; NR: non-reducing; MFI: mean fluorescent intensity

TGN1412 were analyzed in a serial dilution, and both showed binding to human T cells with EC_{50} values of 4.9 nM and 2.5 nM, respectively [Figure 1C]. Only E1P2 exhibited binding to mouse T-cells with an EC_{50} value of 88 nM, which is approximately 18-fold lower than its EC_{50} value toward human T cells. To exclude any nonspecific binding of the newly isolated E1P2 clone, different CD28-negative cell lines were screened by flow cytometry [Supplementary Figure S6]. No cell binding was observed in that setting, highlighting the specificity of E1P2 to CD28.

Epitope mapping reveals a different binding epitope of E1P2 than TGN1412

The crystal structure of 5.11A1, a precursor mAb of TGN1412, revealed a lateral binding to an epitope close to the cell surface membrane [Figure 2A, PDB: 1YJD].⁴⁷ To confirm that E1P2 does not bind to the same region as superagonistic antibodies, we used SPOT technology⁴⁸ to map the antibody's epitope [Supplementary Table 1]. E1P2 binds to a conformational epitope near the apex of CD28 and close to the binding region

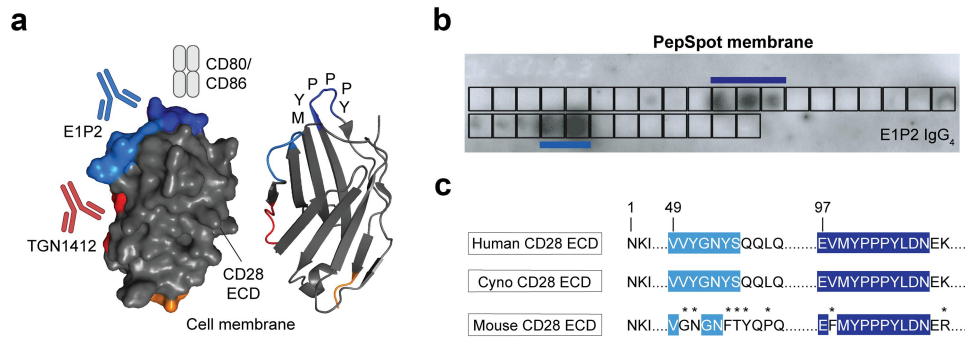


Figure 2. Epitope mapping of E1P2 using SPOT technology. (a) The binding regions of E1P2 (highlighted in light and dark blue) are different from that of TGN1412 (highlighted in red). (b) A cellulose membrane with overlapping peptides covering the ECD of human CD28 was used to highlight the binding epitope. E1P2 binds to the apex of CD28 close to the natural binding site of CD80/CD86 (near the MYPPPY region), unlike TGN1412, which was previously shown to bind to a lateral epitope (PDB: 1YJD). The binding spots of E1P2 on the cellulose membrane show a conformational epitope since two different regions were positive. (c) Sequence alignment of human/cyno/mouse CD28 with the potential binding residues of E1P2 highlighted in blue. The non-identical sequence between human/cyno/mouse CD28 is indicated with an asterisk (*). Cyno: Cynomolgus monkey ECD: extracellular domain

of CD80/CD86 [Figure 2a,b]. The PepSpot assay was also performed using TGN1412, in which the binding region on the cellulose membrane matched with the published crystal structure for superagonistic antibodies [Supplementary Figure S7]. Since the CD28 sequence is naturally conserved between humans and cynomolgus monkeys, E1P2 displays a specific binding to human and cynomolgus monkey CD28 [Figure 2c].

E1P2 does not activate human PBMCs in the absence of TCR/CD3 stimulation

After confirming that E1P2 was binding to a different epitope than TGN1412, an *in vitro* activity assay on human PBMCs was performed to exclude any undesired superagonistic properties. Superagonistic mAbs against CD28 activate T cells in the absence of signal 1, via clustering of CD28

[Figure 3A].³⁴ E1P2, TGN1412, and isotype control in IgG₄ format were wet-coated on 6-well plates, and freshly thawed human PBMCs from a healthy donor were added. As expected, the superagonistic TGN1412 antibody induced proliferation of PBMCs, secretion of pro-inflammatory cytokines (IL-2, IFN- γ , and TNF- α), and expression of an early activation marker (CD69) and a late activation marker (CD25) mainly on CD4⁺ T-cells [Figure 3B-D]. None of these effects were observed with E1P2, suggesting that the new anti-CD28 antibody has no superagonistic characteristics. These assays were performed on PBMCs from two other healthy donors to evaluate inter-donor variability, showing comparable trends [Supplementary Figure 8, A and B]. Since E1P2 cross-reacts with mouse CD28, an *in vitro* superagonistic assay was also performed with mouse T cells, and no sign of T-cell activation was observed [Supplementary Figure 8C].

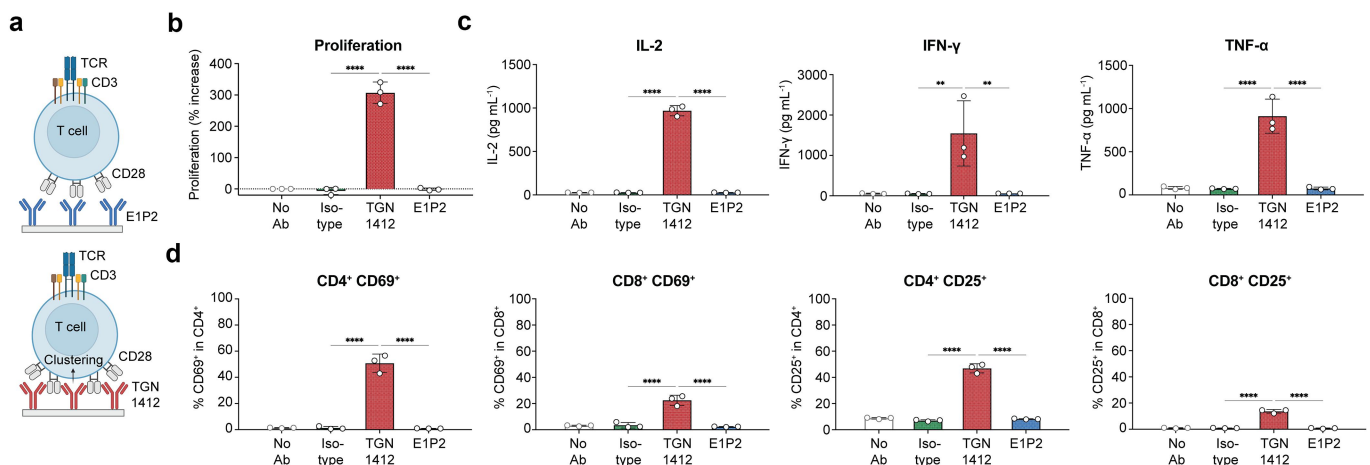


Figure 3. In vitro superagonistic assay on human PBMCs. (a) A graphical representation for the binding mode of conventional mAbs like E1P2 (top) and superagonistic mAbs like TGN1412 (bottom). Antibodies were wet coated on 6-well plates (6 μ g/well), and human PBMCs from a healthy donor were added (1.5 million/well). (b) A significant proliferation of PBMCs was observed using an MTS assay in the presence of TGN1412, but not E1P2, after 5 days. (c) Different pro-inflammatory cytokines (IL-2, IFN- γ , and TNF- α) were quantified by ELISA after 3 days. No cytokines were elevated after adding E1P2, unlike TGN1412. (d) The expression of an early activation marker (CD69) and a late activation marker (CD25) was assessed by flow cytometry on CD4⁺ and CD8⁺ T cells after 3 days. Activation markers were only elevated in the presence of TGN1412, but not E1P2. Data are presented as mean \pm SD. Each dot represents the value of a technical replicate. Statistical analysis of the data was performed by one-way ANOVA followed by Tukey's multiple comparison test. * p <0.05; ** p <0.01; *** p <0.001; **** p <0.0001.

Co-stimulation assay of E1P2 with an anti-CD3 IgG

Conventional anti-CD28 mAbs provide a strong co-stimulation for T-cell activation if signal 1 is also present. To examine if E1P2 has this desired property, a co-stimulation assay on human PBMCs was performed. An anti-CD3 IgG₄ (clone: OKT3) was wet-coated on six-well plates. E1P2, TGN1412, and an isotype control in IgG₄ and freshly thawed human PBMCs were added to the solution [Figure 4A]. E1P2, combined with OKT3, mediated a significant proliferation of human PBMCs with a 2-fold increase compared to OKT3 plus isotype control [Figure 4B]. IL-2 is a crucial cytokine that drives T-cell expansion and differentiation.^{49,50} While low levels of IL-2 were produced in the presence of OKT3 only, the combination with E1P2 resulted in a 100-fold increase in IL-2 secretion [Figure 4C]. This co-stimulation effect was more potent with E1P2 than TGN1412, suggesting different epitopes might have different agonistic properties. Other important cytokines were also significantly induced with the E1P2 combination: a 10-fold increase in IFN- γ and a 5-fold increase in TNF- α were observed. These results were also confirmed in two additional healthy donors, where E1P2 provided a strong costimulatory signal through enhancing IL-2 secretion when combined with OKT3 [Supplementary Figure S9, A and B]. E1P2 induced a significant increase in proliferation and IL-2 production in mouse T-cells when combined with an anti-mouse CD3 (clone: 2C11, Supplementary Figure S9C). Collectively, these data confirm that E1P2 only provides strong co-stimulation in the presence of signal 1 from anti-CD3 mAbs.

E1P2 synergizes with an anti-CD3/anti-EDB BiTE

CD3-targeting BiTEs can elicit an anti-tumor response by bridging cytotoxic T cells to cancer cells. However, the absence of a costimulatory signal can limit T-cell activity due to early exhaustion and lack of proliferation. We investigated the synergistic effect of combining IgG₄ (E1P2) with an anti-CD3 BiTE targeting extracellular domain B (EDB), a validated tumor target [Figure 4D]. EDB is a stromal target that is highly expressed in a variety of tumors.⁵¹ The amino acid sequence and the quality control of the BiTE are shown in Supplementary Figure S10. Human PBMCs were incubated with EDB⁺ WI-38 cells in a 5 to 1 ratio (effector-to-target) and different concentrations of anti-CD3/anti-EDB BiTE (0, 0.1, 1, and 10 nM) in the presence or absence of IgG₄ (E1P2) or TGN1412 (50 nM). The anti-CD3 BiTE alone induced moderate target cell lysis at concentrations of 1 and 10 nM (33% and 47% of dead cells, respectively), and no effect was observed at concentrations of 0 and 0.1 nM [Figure 4E]. The combination of IgG₄(E1P2) with an anti-CD3 BiTE doubled the percentage of target cell lysis. This synergistic effect was only observed at CD3 BiTE concentrations that were initially active when added as a single agent (i.e., 1 and 10 nM), highlighting that, unlike TGN1412, E1P2 only shows activity in the presence of CD3 signaling. Similar results were also obtained when assessing CD25 expression, IFN- γ release, and T-cell proliferation [Figure 4F-H].

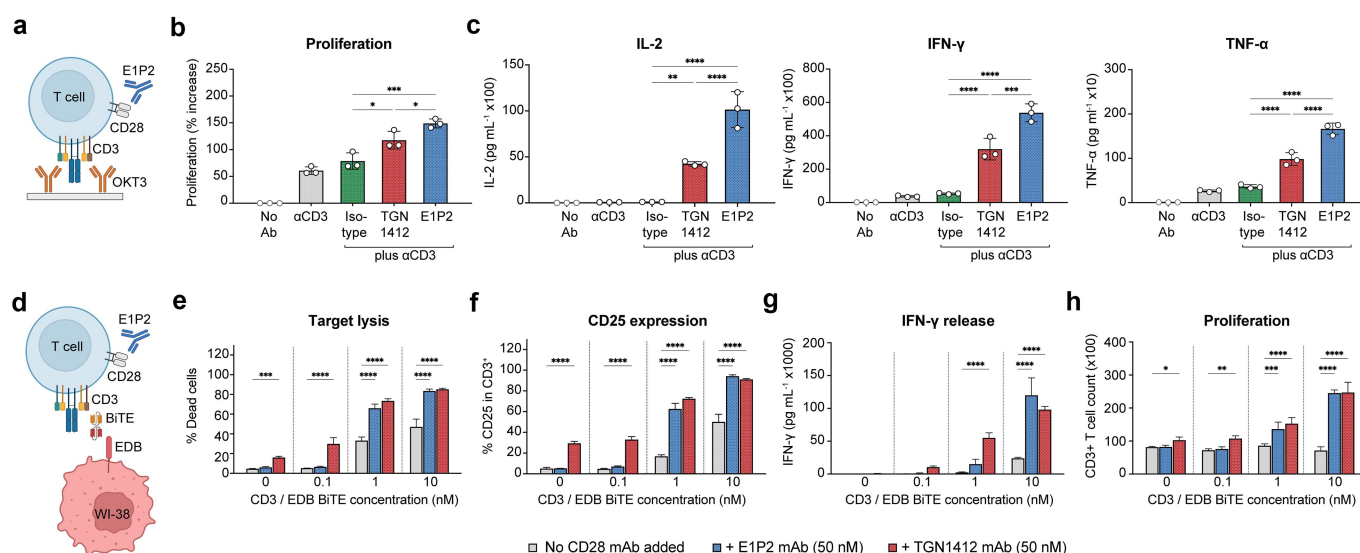


Figure 4. In vitro co-stimulation assay with anti-CD3 antibodies. Freshly thawed human PBMCs from a healthy donor were used to test the activity of IgG₄(E1P2) in combination with either an anti-CD3 mAb (OKT3) or an anti-CD3/anti-EDB BiTE. (a) OKT3 was wet coated on 6-well plates (2 μ g/well), and antibodies (E1P2 IgG₄, TGN1412, or isotype control) were added to the solution (15 μ g/well) with human PBMCs. (b) A 2-fold increase in cell proliferation was observed when IgG₄(E1P2) was combined with OKT3, in comparison to when an isotype control was combined with OKT3. (c) Minimal secretion of cytokines was seen when adding OKT3 alone to human PBMCs, especially IL-2. A 100-fold increase in IL-2 secretion, a 10-fold increase in IFN- γ secretion, and a 5-fold increase in TNF- α were observed when combining IgG₄(E1P2) with OKT3. (d) EDB⁺ WI-38 cells were used as target cells to examine the synergistic effect in an *in vitro* killing assay. Human PBMCs were added (effector to target ratio of 5:1) in the presence of different concentrations of anti-CD3/anti-EDB BiTE, and in the presence or absence of IgG₄(E1P2) or controls. (e-h) A potent synergistic effect was observed as reflected in target cell lysis, CD25 expression, IFN- γ release, and cell proliferation. The activity seen with IgG₄(E1P2) was only in combination with CD3 bispecific antibodies, unlike the superagonistic TGN1412 antibody that showed nonspecific activation. Data are presented as mean \pm SD ($n=3$ from technical replicates). Statistical analysis of the data was performed by one-way ANOVA followed by Tukey's multiple comparison test (B&C) or by two-way ANOVA followed by Dunnett's multiple comparison test (E-H). * $p < 0.05$; ** $p < 0.01$; *** $p < 0.001$; **** $p < 0.0001$.

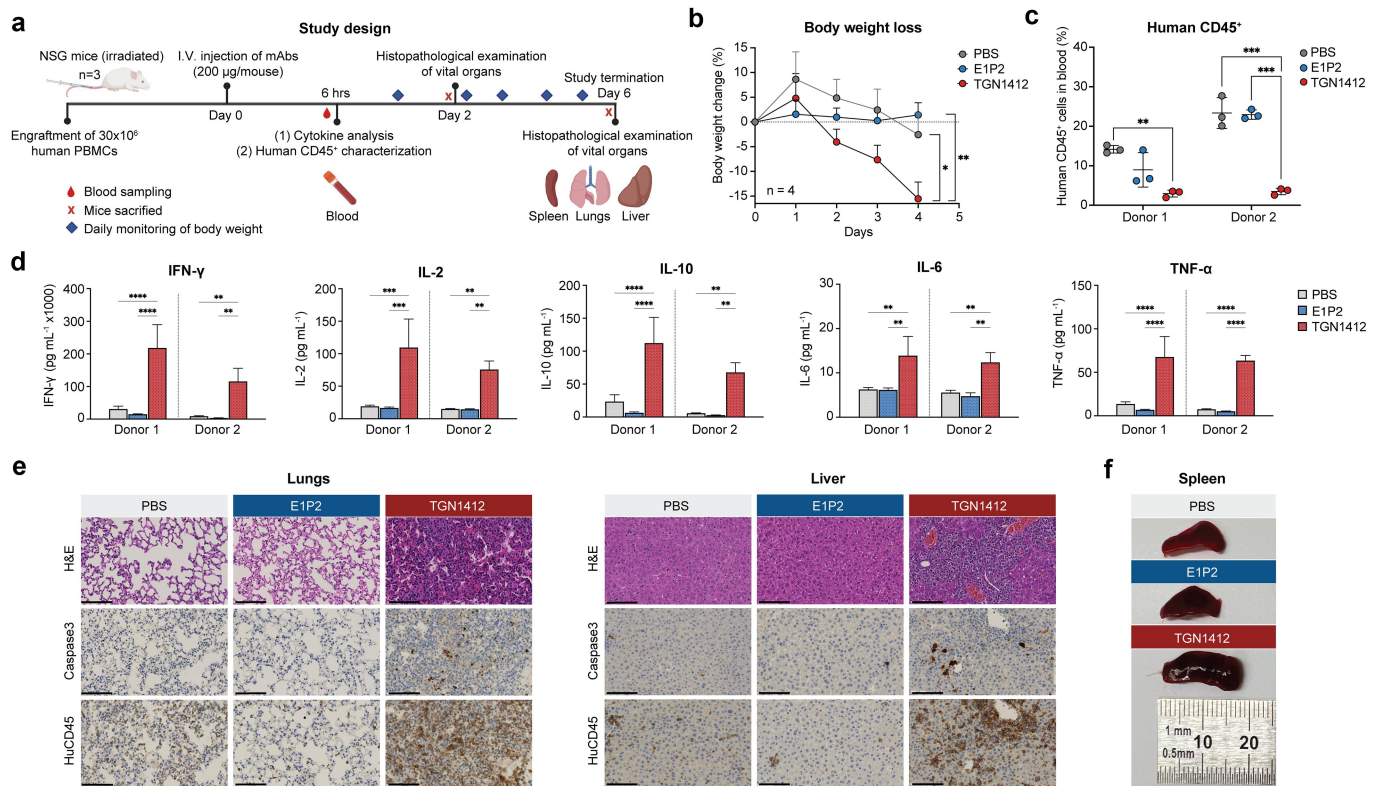


Figure 5. In vivo safety study in humanized NSG mice. (a) The study design for the *in vivo* toxicity experiment highlighting the important milestones. NSG mice were humanized by engrafting 30×10^6 human PBMCs from two different healthy donors. IgG₄(E1P2), TGN1412, or PBS were injected, and a blood sample was taken after 6 hours to measure serum cytokines and to characterize the human CD45⁺ population. After 2 and 6 days, mice were sacrificed, and organs were examined for histopathological findings. (b) The TGN1412 group exhibited severe body weight loss upon treatment. (c) The human CD45⁺ population rapidly declined after the administration of TGN1412, but not E1P2. (d) Serum cytokines were quantified after 6 hours, and significant elevation was observed after injecting TGN1412, unlike E1P2. (e) Histopathological examination of vital organs after 6 days using H&E, Caspase3, and human CD45 staining. Necrotic tissues were observed in the TGN1412 group, but not in the E1P2 group. (f) The size of the spleen was measured by a ruler after 2 days, and splenomegaly was observed only after administering TGN1412. Representative data from two mice are shown in E and F. Data are presented as mean \pm SD ($n=3$ from technical replicates, except in B in which $n=4$ from biological replicates). Statistical analysis of the data was performed by two-way ANOVA followed by Dunnett's multiple comparison test (B-D). * $p < 0.05$; ** $p < 0.01$; *** $p < 0.001$; **** $p < 0.0001$. Scale bar: 100 μ m. * $p < 0.05$; ** $p < 0.01$; *** $p < 0.001$; **** $p < 0.0001$. Scale bar: 100 μ m.

E1P2, in contrast to TGN1412, does not show signs of toxicity in humanized NSG mice

To further confirm that E1P2 has no superagonistic properties, an *in vivo* safety study was conducted in NSG mice injected with human PBMCs from 2 different healthy donors [Figure 5A]. Five days after PBMCs engraftment, mice were injected with IgG₄(E1P2), TGN1412, or phosphate-buffered saline (PBS). Daily monitoring of behavior and body weight revealed apparent pain symptoms and severe body weight loss in mice treated with TGN1412, which was not observed upon treatment with E1P2 [Figure 5B]. Six hours after mAb administration, a blood sample was taken to measure the percentage of human CD45⁺ cells in the blood and to quantify serum cytokines. Mice treated with TGN1412 exhibited a rapid decrease in human CD45⁺ cells in the blood and substantially increased serum levels of multiple pro-inflammatory cytokines (i.e., IL-2, IL-6, IL-10, IFN- γ , and TNF- α) [Figure 5c,d]. None of these effects were observed upon treatment with E1P2 or PBS. To examine any potential organ damage exerted by the treatment, a histopathological analysis of the lungs and liver was conducted after 6 days. In the TGN1412 group, hematoxylin and eosin (H&E) staining showed signs of necrotic tissues, which was also confirmed with Caspase3 staining [Figure 5E].

These results were also reflected in the infiltration of human CD45⁺ cells in the lungs and liver. Splenomegaly was only observed in mice treated with TGN1412 [Figure 5F]. Overall, E1P2 did not show any signs of organ damage or CRS in strong contrast to TGN1412.

Discussion

In this work, we described the generation and *in vivo* safety validation of a novel fully human antibody targeting CD28, a critical costimulatory receptor that provides signal 2 required for full T-cell activation. It is well-established that CD28 costimulation profoundly enhances the anti-tumor activity in the presence of signal 1 from the TCR/CD3 complex.⁵² For instance, the incorporation of costimulatory domains, such as CD28, into first-generation CAR T cells has led to remarkable anti-tumor response against hematological malignancies (e.g., Yescarta[®] for diffuse large B cell lymphoma).^{26–29} While CAR T-cells are considered to be one of the most potent cancer therapies in the market, their development is often challenging due to the laborious preparation and individual customization. In principle, antibody-based therapeutics targeting CD28 would have the advantage of being off-the-shelf pharmaceuticals.

Inspired by the crucial role of CD28, the TeGenero trial in 2006 using a CD28-activating mAb (TGN1412) was initiated, but it resulted in a clinical tragedy in which all six healthy volunteers who received the drug developed CRS with severe life-threatening complications.³³ This incident halted further development of anti-CD28 mAbs and raised safety concerns. Therefore, there is a need for new mAbs against CD28 that have different properties and are safe for clinical use. We isolated “E1P2”, a novel fully human anti-CD28 mAb, using phage display technology. We aimed to favor binders toward the apex of CD28 by masking the superagonistic TGN1412 epitope through the attachment of the biotin-streptavidin-magnetic bead complex close to this region. An alternative strategy would have been to include TGN1412 in the panning rounds in order to block that site during the selection process. E1P2 binds to both human and mouse CD28, as shown by flow cytometry on primary T cells. This critical feature facilitates the preclinical testing of E1P2 before further clinical development, considering the preclinical failure to predict toxicity from TGN1412.^{33,39,40}

The superagonistic property of TGN1412, i.e., the polyclonal activation of T cells via CD28 cross-linking without signal 1, was later found to cause severe side effects at the human-tested dose.^{34,37,38} Our aim was to generate mAbs that can provide a potent costimulatory signal, mimicking the natural ligands (i.e., only in the presence of TCR/CD3 stimulation). In comparison to TGN1412, IgG₄(E1P2) did not activate human PBMCs *in vitro* when coated on tissue culture plates. This was confirmed through: 1) the absence of cytokine release (IL-2, IFN- γ , and TNF- α); 2) no observed induction of cell proliferation; and 3) the lack of expression of activation markers like CD69 and CD25 on CD4⁺ and CD8⁺ T-cells. Blood samples of three healthy donors were tested, confirming that E1P2 does not exhibit superagonistic properties across different donors. The lack of superagonistic properties for E1P2 may be attributed to the different binding epitope of E1P2 than TGN1412, as we showed in the epitope mapping using SPOT technology. A limitation of the *in vitro* superagonistic assay is that the mAbs had to be artificially coated on a solid support.⁵³ Alternatively, humanized NSG mice have been shown to be sensitive to predicting the toxicity of immunotherapeutic agents, including TGN1412, retrospectively.⁴⁴ We adapted this model and successfully demonstrated that only TGN1412, but not E1P2, showed: 1) CRS with different pro-inflammatory cytokines after 6 hrs; 2) severe body weight loss; 3) signs of vital organ damage (lungs and liver); 4) splenomegaly; and 5) rapid loss of human CD45⁺ cells from the blood, with subsequent organ infiltration. While human PBMCs can be rapidly engrafted in NSG mice, graft-versus-host disease often develops within 3–4 weeks.⁵⁴ This can limit long-term safety assessments, which is important in the context of immunotherapy.

After assessing the safety profile, we tested the potential synergistic effect of IgG₄(E1P2) in combination with an anti-CD3 BiTE targeting EDB as proof of concept for efficacy. EDB is a selective tumor marker, and our group has developed various antibody-based therapeutics that are currently being investigated in clinical trials.^{55–57} We showed that the combination significantly improved the target cell lysis (2-fold

increase), compared to the anti-CD3 BiTE alone. The combination also led to a more than 3-fold increase in T-cell proliferation, which is crucial for sustained anti-tumor activity. Importantly, this activity of E1P2 was only found in the presence of the anti-CD3 BiTE, unlike the nonspecific activity observed with TGN1412. These data are in line with what Laszlo *et al.* reported for their combination of a conventional anti-CD28 mAb with an anti-CD3/anti-CD33 BiTE (AMG 330) against AML.³⁰ In principle, CD28 binding with suitable IgG reagents may boost the activities of endogenous tumor-infiltrating lymphocytes or CD3-targeting bispecific antibodies, similar to what is observed with immune checkpoint blockers (e.g., anti-PD-1). However, the lack of tumor-targeting properties of an anti-CD28 antibody may potentially lead to nonspecific activation of autoreactive T cells. To overcome this limitation, CD28-targeting bispecific antibodies are being considered to boost CD3 bispecific antibodies, which can also enhance tumor selectivity if different target epitopes are chosen. For example, REGN5668 targeting Muc16 in ovarian cancer is currently being tested in clinical trials.^{31,32}

To our knowledge, E1P2 is the first fully human mAb that cross-reacts with human, mouse, and cynomolgus monkey CD28. The unique binding property of E1P2 contributed to the strong costimulatory effect, but only in the presence of a signal 1 from the TCR/CD3 complex, unlike TGN1412. We anticipate that E1P2 may serve as a useful modular building block for the design of immunostimulatory antibody therapeutics, which boost anti-tumor response only in the presence of signal 1 and without the nonspecific superagonistic properties of TGN1412-like reagents. A number of bispecific antibodies based on E1P2 have been generated and are currently being evaluated for their therapeutic activity.

Materials and methods

Cell lines

Buffy coats from healthy blood donors were obtained from the Zurich blood donation service (Blutspende Zurich, Switzerland). PBMCs were isolated by density centrifugation using Ficoll-Paque plus (GE Healthcare). Primary T cells were separated by negative selection using EasySep™ Human T-cell isolation kit according to the manufacturer's instructions (STEMCELL™ Technologies). PBMCs and T cells were cryopreserved in freezing media (90% fetal bovine serum (FBS) with 10% dimethylsulfoxide) and stored in liquid nitrogen before use. For cell culture, T-cell media was prepared using Advanced RPMI 1640 supplemented with 10% FBS, 1% Penicillin-Streptomycin, and 1% GlutaMAX™; all components were purchased from Gibco™. Primary mouse T cells were isolated from the spleen of a BALB/c mouse bearing a subcutaneous CT26 tumor by negative selection using EasySep™ Mouse T-cell isolation kit. CHO cells and WI-38 human fibroblasts were obtained from ATCC and expanded according to the manufacturer's protocol. Authentication of the cell lines, including the evaluation of post-freeze viability, growth properties, morphology, test for mycoplasma contamination, isoenzyme assay, and sterility tests, was performed by the cell bank before shipment. WI-38 cells were modified to

genetically express eGFP using a second-generation lentiviral system as previously described.⁵⁸

Production of recombinant CD28-Fc fusion protein

The gene encoding for the ECD of human CD28 with C-terminal AviTag™ (biotin ligase recognition sequence), 6× Histidine tag, and a human IgG₁ Fc was cloned into the mammalian expression vector pcDNA3.1(+). An enterokinase cleavage site was incorporated before the Fc tag to potentially isolate the CD28 moiety from the Fc fusion. The protein was produced in CHO-S cells by transient gene expression (TGE) as previously described.⁵⁹ Purification was performed by protein A affinity chromatography and SEC on a Superdex 200 increase 10/300 GL (GE Healthcare) to obtain a monomeric fraction. Site-specific enzymatic biotinylation was done using *E. coli* biotin ligase (BirA), as described before.⁶⁰ The quality and functionality of the recombinant protein were assessed by SEC, SDS-PAGE, and ELISA using a commercial anti-CD28 mAb (clone: CD28.2, Biolegend; 302902).

Isolation of E1P2 by phage display

The synthetic AMG phage display library was used to isolate fully human antibodies against the recombinant human CD28 Fc fusion protein, following the protocol described previously by Viti et al.⁶¹ Briefly, the biotinylated human CD28 Fc fusion antigen (120 pmol) was incubated with 60 μ L of streptavidin-coated magnetic beads (M280, Invitrogen). ScFvs-displaying phage from the AMG library were incubated for 2 hours with an excess of nonspecific human IgG₁ to saturate potential binders against the human Fc portion. The phage library was then added to the immobilized antigen (pre-blocked with 4% milk-PBS). After several washes with PBS and PBS-Tween 20 (0.1%), bound phage was eluted using triethylamine, and helper phage (VCS-M13) was used to amplify the clones in *E. coli* TG-1. Subsequently, another round of biopanning was performed. At the end of the selection, expression of scFvs from individual clones in 2×YT media was induced through the addition of 1 mM IPTG and overnight incubation at 30°C. Clones were screened for binding by ELISA against human CD28 Fc fusion. To exclude binders against the Fc domain, a second ELISA was performed in parallel against human IgG₁. CD28 binding clones were sequenced and used for further characterization. Clones were reformatted into an IgG₄ backbone plasmid (pMM137, in-house) and produced in CHO-S cells by TGE for further characterization. TGN1412 was produced in-house and used as a positive control.

Binding validation by ELISA

To evaluate the binding properties of IgG₄(E1P2), ELISA was performed on both human and mouse CD28 Fc fusion proteins. Briefly, 100 nM of the biotinylated proteins were immobilized on streptavidin-coated wells for 1 hour. To confirm specificity, an irrelevant protein was used as a negative control. After blocking with 4% milk-PBS for 2 hours, fluorescein isothiocyanate (FITC)-labeled IgG₄(E1P2) or TGN1412 were added in a serial dilution in triplicates. For detection,

a secondary rabbit anti-FITC antibody (Bio-Rad; 4510–7604) was added, followed by goat anti-rabbit IgG conjugated to horseradish peroxidase (HRP; Sigma; A6154). The colorimetric reaction was developed using a POD substrate (Roche). Absorbance at 450 nm was measured on a microplate reader (Tecan). A sigmoid curve for antibody concentration (x-axis) against absorbance (y-axis) was plotted and fitted using a 4-parameter logistic (4PL) non-linear regression model to calculate the EC₅₀ values. The binding of scFv (E1P2) was also evaluated by ELISA. ScFv(E1P2), featuring a c-myc-tag, was added to the coated CD28 Fc fusion protein in a serial dilution. Mouse anti-c-myc (Clone: 9E10) was added, followed by goat anti-mouse IgG (Fc-specific) conjugated to HRP (Sigma; A0168). The colorimetric reaction was developed, and data were analyzed as mentioned above.

Binding validation by flow cytometry

Flow cytometry was performed in a serial dilution to validate the binding of IgG₄(E1P2) to primary human and mouse T-cells by three independent flow cytometry measurements. TGN1412 and an isotype IgG₄ were used as controls. T cells (200'000 cells per well) were first blocked with fluorescence-activated cell sorting (FACS) buffer (PBS, 2% bovine serum albumin, and 2 mM EDTA) for 30 minutes. Different dilutions of primary antibodies were added to cells and incubated for 45 minutes at 4°C. After two washing steps using FACS buffer, goat anti-human IgG Fc secondary antibody conjugated to phycoerythrin (PE; (Invitrogen; 12-4998-82) was added and incubated for 30 minutes at 4°C in the dark. After two washes with PBS, Zombie Violet live/dead staining (Biolegend) was added and incubated for 30 minutes at 4°C in the dark. Data were acquired on a Cytotflex S flow cytometer (Beckman Coulter) and analyzed using the FlowJo software v10 (BD Biosciences). Mean fluorescent intensity (MFI) was determined, and the sigmoid curve for antibody concentration (x-axis) against relative MFI (y-axis) was plotted and fitted using a 4-parameter logistic (4PL) non-linear regression model in order to calculate the EC₅₀ values.

Epitope mapping using peptide array

Overlapping peptides (15 amino acid-long) covering the extracellular domain sequence of the human CD28 were purchased from JPT (SPOT synthesis). The peptides were covalently bound to a cellulose membrane on 32 different spots. Before the first use, the membrane was rinsed with 30 ml methanol for 5 minutes to avoid precipitation of hydrophobic peptides during the following washing procedure. Then, the membrane was washed three times for 3 minutes with 50 mL of TBS-T buffer (50 mM TRIS; 137 mM NaCl; 2.7 mM KCl; 0.05% Tween 20; pH 8.0). To reduce the background signal, the membrane was blocked in 5% Milk-PBS at 4°C overnight while gently shaking. The membrane was incubated with 5 μ g/ml of IgG₄(E1P2) in 5% milk-PBS for 3 hours at room temperature with gentle shaking, followed by a secondary anti-human Fc specific conjugated to HRP (Sigma; A0170). The washing steps in TBS-T were repeated three more times for five minutes. In a dark room, the membrane was incubated with 2 ml of Amersham

ECL start Western blotting detection reagent (GE Healthcare) and developed according to the manufacturer's instructions. The potential binding region of E1P2 was aligned on the published crystal structure of 5.11A1 (PDB: 1YJD),⁴⁷ a precursor mAb of TGN1412, to highlight the potential binding epitope of E1P2.

In vitro superagonistic assay

IgG₄(E1P2), TGN1412, or isotype control were coated on 6-well tissue culture plates at a concentration of 3 µg/ml in PBS (2 ml/well) for 2 hours at 37°C and 5% CO₂. Uncoated wells were used as a negative control. The antibody solution was then aspirated from each well without any washing steps. Freshly thawed human PBMCs were added at a concentration of 0.5 million/ml (3 ml/well) in T-cell media and incubated for 3 or 5 days. The experiment was performed in triplicates, using three different healthy donors. For the proliferation assay, 200 µL from each well was transferred after 5 days to a flat-bottom microplate, and a colorimetric MTS assay was performed as described by the manufacturer (Promega). For the activation assay, cells were pelleted after 3 days, and flow-cytometric analysis was done to determine the expression level of activation markers using the following panel: anti-human CD4 FITC, anti-human CD8 BV421, anti-human CD69 PE, anti-human CD25 Alexa Fluor® 647, and Zombie Violet live/dead staining (Biolegend). For the cytokine analysis, the supernatant was extracted after 3 days, and the level of secreted IL-2, IFN-γ, and TNF-α was quantified using Biolegend's ELISA Max™. For mouse T-cells, antibodies were coated at a concentration of 5 µg/ml, and assays were performed as described above using the following panel for flow cytometry: anti-mouse CD3 FITC, anti-mouse CD25 APC/Cy7, and anti-mouse CD69 PE. A list of the antibody clones used for flow cytometry is shown in Supplementary Table 2.

In vitro co-stimulation assay with an anti-CD3 IgG

Anti-human CD3 IgG₄ (clone: OKT3, produced in-house) was coated on 6-well tissue culture plates at a concentration of 1 µg/ml in PBS (2 ml/well) for 2 hours at 37°C and 5% CO₂ before being aspirated. IgG₄(E1P2), TGN1412, or isotype control were added to the solution at a concentration of 5 µg/ml. Human PBMCs were added as previously described, and proliferation, as well as cytokine release, were measured after 3 days. The assays were conducted in a similar way with mouse T cells using a concentration of 5 µg/ml of anti-mouse CD3 (clone: 2C11, Biolegend).

In vitro co-stimulation assay with CD3 bispecific antibodies

WI-38 cells expressing the fibronectin EDB and eGFP were coated on a 96-well plate (20'000 cells/well). Freshly frozen human PBMCs (effector cells) were added to obtain an effector-to-target ratio of 5 to 1. Different concentrations of anti-CD3/anti-EDB BiTE were added (clone SP-34 for the anti-CD3 and clone L19 for the anti-EDB) in a 10-fold serial dilution (10, 1, and 0.1 nM). A condition of no added BiTE was also included

as a negative control. E1P2 and TGN1412 IgG₄ at a fixed concentration of 50 nM were added to each condition. After 4 days, cells were detached using an Accutase® Cell detachment solution. The supernatant was collected to measure the level of IFN-γ release by ELISA. The remaining pellet and debris were washed with PBS before staining with Zombie Violet live/dead staining (Biolegend) and incubated for 30 minutes at 4°C in the dark. Cells were washed once with FACS buffer and stained with an antibody master mix containing anti-human CD3 APC and anti-human CD25 Alexa Fluor® 647. Target cells were discriminated from effector cells via their eGFP expression, and the percentage of dead cells was calculated by gating on dead cells. The absolute count of live CD3⁺ T-cells was calculated to assess the proliferation. The percentage of CD25 expression on CD3⁺ T-cells was also assessed.

In vivo safety study in NSG mice

Humanized mice were generated by engrafting 30 × 10⁶ PBMCs from 2 different healthy donors intravenously in eight-week-old female NSG mice (NOD.Cg-Prkdc^{scid} Il2rg^{tm1Wjl}/SzJ). NSG mice were first irradiated sub-lethally with 150 cGy (RS-2000 irradiator, Rad Source, Buford, GA, USA) 5 hours before PBMCs engraftment. After 5 days, mAbs (200 µg/mouse) were injected intravenously. Tail-tip blood sampling was performed 6 hours post-mAb injection. For serum preparation, the samples were left to clot at room temperature for 2 hours, then spun down at 2,000 g for 30 minutes before freezing. Cytokine analysis was performed using MSD® U-PLEX human Biomarker Group 1 (IL-2, IL-6, IL-10, IFN-γ, and TNF-α), and an electrochemiluminescence signal was acquired using an MSD® instrument. For flow cytometry, blood was collected in EDTA tubes (FisherScientific), and red blood cells were removed using RBC lysis buffer (BioLegend). Cells were pelleted and washed with PBS before staining with Zombie Red live/dead staining (Biolegend), and incubated for 30 minutes at 4°C in the dark. Cells were washed once with FACS buffer and then stained with anti-human CD45 PerCP cy5.5 (Biolegend). After 2 days, one mouse/group was sacrificed for histopathological examination of the spleen. The size of the spleen was measured using a ruler. Body weight was monitored daily, and mice were sacrificed when they lost more than 15% of their initial body weight. After 6 days, all mice were sacrificed, and organs (lungs and liver) were examined for histopathological findings.

Histology and immunohistochemistry

Freshly dissected lungs and liver were fixed in 4% buffered paraformaldehyde, decalcified in EDTA for 12 hours, and then paraffin-embedded. Tissues were cut (3 µm) and mounted on SuperFrost™ slides (Thermo Fisher Scientific, Waltham, USA). The murine tissues were processed by the Department of Pathology, University Hospital Zurich. Conventional staining with H&E was performed on all slides to assess tissue cellularity, morphology, and necrosis. For immunohistochemistry (IHC), slides were stained with primary antibodies directed against human CD45 and murine Caspase3. Slides were stained with the Ventana Optiview platform (Ventana Medical Systems, Inc, Tucson, AZ, USA) according to the

manufacturer's protocols. Specimens were analyzed by light microscopy (Axioskop 40, Zeiss, Oberkochen, Germany) and scanned images (Nano Zoomer C9600 Virtual Slide Light microscope scanner and NDP View Software, version 1.2.36, both Hamamatsu Photonics K.K., Hamamatsu City, Japan). All staining intensities were compared to isotype controls.

Statistical analysis

All experiments were performed in triplicates unless specified differently. Data were analyzed using GraphPad Prism software (v9) and are represented as mean \pm SD. Statistical analysis of the data was performed by one-way ANOVA followed by Tukey's multiple comparison test or two-way ANOVA followed by Dunnett's multiple comparison test. Statistical significance was considered for P-values below 0.05. * $p < 0.05$; ** $p < 0.01$; *** $p < 0.001$; **** $p < 0.0001$.

Abbreviations

AML	Acute myeloid leukemia
APC	Antigen-presenting cell
BiTE	Bispecific T-cell engager
CAR	Chimeric antigen receptor
CHO	Chinese hamster ovary
CRS	Cytokine release syndrome
EDB	Extracellular domain B
ECD	Extracellular domain
EM	Effector memory
FACS	Fluorescence-activated cell sorting
FBS	Fetal bovine serum
H&E	Hematoxylin and eosin
HRP	Horseradish peroxidase
MAb	Monoclonal antibody
MFI	Mean fluorescent intensity
MHC	Major histocompatibility complex
PBMC	Peripheral blood mononuclear cell
PBS	Phosphate-buffered saline
ScFv	Single-chain variable fragment
SEC	Size exclusion chromatography
TCR	T-cell receptor
TGE	Transient gene expression

Acknowledgments

We would like to thank Innosuisse Innovation (Project number 55003.1) for their support, in part, in performing the *in vivo* safety study. The authors thank Mattia Matasci for his help with experimental procedures.







Disclosure statement

Dario Neri is a co-founder and shareholder of Philogen (www.philogen.com), a Swiss-Italian Biotech company that operates in the field of ligand-based pharmacodelivery. Abdullah Elsayed, Louis Plüss, Frederik Peisert, Gudrun Thorhallsdottir, Jacqueline Mock, Sheila Dakhel Plaza, Emanuele Puca, and Roberto De Luca are employees of Philochem AG, a daughter company of Philogen acting as the discovery unit of the group.

Funding

The *in vivo* safety study was partially supported by Innosuisse Innovation (Project number 55003.1).

ORCID

Abdullah Elsayed  <http://orcid.org/0000-0001-7080-0853>
 Christian Pellegrino  <http://orcid.org/0000-0001-7898-9988>
 Gudrun Thorhallsdottir  <http://orcid.org/0009-0005-0604-7728>
 Jacqueline Mock  <http://orcid.org/0000-0002-4618-1113>
 Emanuele Puca  <http://orcid.org/0000-0002-2869-3203>
 Roberto De Luca  <http://orcid.org/0000-0001-7519-8689>
 Markus G. Manz  <http://orcid.org/0000-0002-4676-7931>
 Cornelia Halin  <http://orcid.org/0000-0002-7899-2850>
 Dario Neri  <http://orcid.org/0000-0001-5234-7370>

Availability of data and materials

Most of the data that supports the findings of this study are available in the supplementary material of this article. The remaining data that support the findings of this study are available from the corresponding author upon reasonable request.

Author contributions

Conception and design of the project: AE, RDL, and DN; Analysis and interpretation of the data: AE, CP, GT, SDP, AV, JM, and DN; Generation and acquisition of data: AE with inputs of CP, LP, FP, RB, FU, EP and DN; Study methodology: AE, RDL, MGM, CH, and DN. Statistical analysis: AE and DN. Writing, reviewing, and editing were performed by AE and DN with inputs from CP, LP, FP, EP, RDL, MGM, and CH. Study supervision: EDL, MGM, CH, and DN.

Ethical statement

Animal experiments were conducted according to the protocols approved by the Cantonal Veterinary Office Zurich (license number 194/2018) in compliance with the Swiss Animal Protection Act (TSchG) and the Swiss Animal Protection Ordinance (TSchV).

References

- Allison JP, McIntyre BW, Bloch D. Tumor-specific antigen of murine T-lymphoma defined with monoclonal antibody. *J Immunol.* 1982;129(5):2293–300. PMID: 6181166. doi:10.4049/jimmunol.129.5.2293.
- Hedrick SM, Cohen DI, Nielsen EA, Davis MM. Isolation of cDNA clones encoding T cell-specific membrane-associated proteins. *Nature.* 1984;308:149–53. doi:10.1038/308149a0. PMID: 6199676.
- Yanagi Y, Yoshikai Y, Leggett K, Clark SP, Aleksander I, Mak TW. A human T cell-specific cDNA clone encodes a protein having extensive homology to immunoglobulin chains. *Nature.* 1984;308:145–49. doi:10.1038/308145a0. PMID: 6336315.
- Davis MM, Bjorkman PJ. T-cell antigen receptor genes and T-cell recognition. *Nature.* 1988;334:395–402. doi:10.1038/334395a0. PMID: 3043226.
- La Gruta NL, Gras S, Daley SR, Thomas PG, Rossjohn J. Understanding the drivers of MHC restriction of T cell receptors. *Nat Rev Immunol.* 2018;18:467–78. doi:10.1038/s41577-018-0007-5. PMID: 29636542.
- Weiss A, Stobo JD. Requirement for the coexpression of T3 and the T cell antigen receptor on a malignant human T cell line. *J Exp Med.* 1984;160:1284–99. doi:10.1084/jem.160.5.1284. PMID: 6208306.

7. Ohashi PS, Mak TW, Van den Elsen P, Yanagi Y, Yoshikai Y, Calman AF, Terhorst C, Stobo JD, Weiss A. Reconstitution of an active surface T3/T-cell antigen receptor by DNA transfer. *Nature*. 1985;316:606–09. doi:10.1038/316606a0. PMID: 4033759.
8. Weiss A, Imboden J, Hardy K, Manger B, Terhorst C, Stobo J. The role of the T3/antigen receptor complex in T-cell activation. *Annu Rev Immunol*. 1986;4:593–619. doi:10.1146/annurev.iy.04.040186.003113. PMID: 2939858.
9. Janeway CA Jr. T-cell development. Accessories or coreceptors? *Nature*. 1988;335:208–10. PMID: 3261842. doi:10.1038/335208a0.
10. Mueller DL, Jenkins MK, Schwartz RH. Clonal expansion versus functional clonal inactivation: a costimulatory signalling pathway determines the outcome of T cell antigen receptor occupancy. *Annu Rev Immunol*. 1989;7:445–80. doi:10.1146/annurev.iy.07.040189.002305. PMID: 2653373.
11. Appleman LJ, Boussiotis VA. T cell anergy and costimulation. *Immunol Rev*. 2003;192:161–80. doi:10.1034/j.1600-065x.2003.00009.x. PMID: 12670403.
12. Jenkins MK, Taylor PS, Norton SD, Urdahl KB. CD28 delivers a costimulatory signal involved in antigen-specific IL-2 production by human T cells. *J Immunol*. 1991;147(8):2461–66. PMID: 1717561. doi:10.4049/jimmunol.147.8.2461.
13. June CH, Ledbetter JA, Gillespie MM, Lindsten T, Thompson CB. T-cell proliferation involving the CD28 pathway is associated with cyclosporine-resistant interleukin 2 gene expression. *Mol Cell Biol*. 1987;7(12):4472–81. PMID: 2830495. doi:10.1128/mcb.7.12.4472-4481.1987.
14. Martin PJ, Ledbetter JA, Morishita Y, June CH, Beatty PG, Hansen JA. A 44 kilodalton cell surface homodimer regulates interleukin 2 production by activated human T lymphocytes. *J Immunol*. 1986;136(9):3282–87. PMID: 3082984. doi:10.4049/jimmunol.136.9.3282.
15. Weiss A, Manger B, Imboden J. Synergy between the T3/antigen receptor complex and Tp44 in the activation of human T cells. *J Immunol*. 1986;137(3):819–25. PMID: 3088111.
16. Damle NK, Mohaghehpour N, Hansen JA, Engleman EG. Alloantigen-specific cytotoxic and suppressor T lymphocytes are derived from phenotypically distinct precursors. *J Immunol*. 1983;131:2296–300. doi:10.4049/jimmunol.131.5.2296. PMID: 6195259.
17. Siokis A, Robert PA, Demetriou P, Dustin ML, Meyer-Hermann M. F-Actin-Driven CD28-CD80 localization in the immune synapse. *Cell Rep*. 2018;24:1151–62. doi:10.1016/j.celrep.2018.06.114. PMID: 30067972.
18. Freeman GJ, Freedman AS, Segil JM, Lee G, Whitman JF, Nadler LM. B7, a new member of the Ig superfamily with unique expression on activated and neoplastic B cells. *J Immunol*. 1989;143(8):2714–22. PMID: 2794510. doi:10.4049/jimmunol.143.8.2714.
19. Freeman GJ, Borriello F, Hodes RJ, Reiser H, Gribben JG, Ng JW, Kim J, Goldberg JM, Hathcock K, Laszlo G, et al. Murine B7-2, an alternative CTLA4 counter-receptor that costimulates T cell proliferation and interleukin 2 production. *J Exp Med*. 1993;178(6):2185–92. doi:10.1084/jem.178.6.2185. PMID: 7504059.
20. Freeman GJ, Gribben JG, Boussiotis VA, Ng JW, Restivo VA Jr., Lombard LA, Gray GS, Nadler LM. Cloning of B7-2: a CTLA-4 counter-receptor that costimulates human T cell proliferation. *Science*. 1993;262:909–11. PMID: 7694363. doi:10.1126/science.7694363.
21. Caux C, Vanbervliet B, Massacrier C, Azuma M, Okumura K, Lanier LL, Banchereau J. B70/B7-2 is identical to CD86 and is the major functional ligand for CD28 expressed on human dendritic cells. *J Exp Med*. 1994;180:1841–47. doi:10.1084/jem.180.5.1841. PMID: 7525840.
22. Singh A, Dees S, Grewal IS. Overcoming the challenges associated with CD3+ T-cell redirection in cancer. *Br J Cancer*. 2021;124:1037–48. doi:10.1038/s41416-020-01225-5. PMID: 33469153.
23. Eshhar Z, Waks T, Gross G, Schindler DG. Specific activation and targeting of cytotoxic lymphocytes through chimeric single chains consisting of antibody-binding domains and the gamma or zeta subunits of the immunoglobulin and T-cell receptors. *Proc Natl Acad Sci U S A*. 1993;90(2):720–24. PMID: 8421711. doi:10.1073/pnas.90.2.720.
24. Brocker T, Karjalainen K. Signals through T cell receptor-zeta chain alone are insufficient to prime resting T lymphocytes. *J Exp Med*. 1995;181(5):1653–59. PMID: 7722445. doi:10.1084/jem.181.5.1653.
25. Till BG, Jensen MC, Wang J, Chen EY, Wood BL, Greisman HA, Qian X, James SE, Raubitschek A, Forman SJ, et al. Adoptive immunotherapy for indolent non-Hodgkin lymphoma and mantle cell lymphoma using genetically modified autologous CD20-specific T cells. *Blood*. 2008;112:2261–71. doi:10.1182/blood-2007-12-128843. PMID: 18509084.
26. Krause A, Guo HF, Latouche JB, Tan C, Cheung NK, Sadelain M. Antigen-dependent CD28 signaling selectively enhances survival and proliferation in genetically modified activated human primary T lymphocytes. *J Exp Med*. 1998;188:619–26. doi:10.1084/jem.188.4.619. PMID: 9705944.
27. Sadelain M, Brentjens R, Rivière I. The basic principles of chimeric antigen receptor design. *Cancer Discov*. 2013;3:388–98. doi:10.1158/2159-8290.Cd-12-0548. PMID: 23550147.
28. Locke FL, Neelapu SS, Bartlett NL, Siddiqi T, Chavez JC, Hosing CM, Ghobadi A, Budde LE, Bot A, Rossi JM, et al. Phase 1 Results of ZUMA-1: a Multicenter Study of KTE-C19 Anti-CD19 CAR T Cell Therapy in Refractory Aggressive Lymphoma. *Mol Ther*. 2017;25:285–95. doi:10.1016/j.yimthe.2016.10.020. PMID: 28129122.
29. Neelapu SS, Locke FL, Bartlett NL, Lekakis LJ, Miklos DB, Jacobson CA, Braunschweig I, Oluwole OO, Siddiqi T, Lin Y, et al. Axicabtagene ciloleucel CAR T-Cell therapy in refractory large B-Cell lymphoma. *N Engl J Med*. 2017;377:2531–44. doi:10.1056/NEJMoa1707447. PMID: 29226797.
30. Laszlo GS, Gudgeon CJ, Harrington KH, Walter RB. T-cell ligands modulate the cytolytic activity of the CD33/CD3 BiTE antibody construct, AMG 330. *Blood Cancer J*. 2015;5:e340. PMID: 26295610. doi:10.1038/bcj.2015.68.
31. Skokos D, Waite JC, Haber L, Crawford A, Hermann A, Ullman E, Slim R, Godin S, Ajithdoss D, Ye X, et al. A class of costimulatory CD28-bispecific antibodies that enhance the antitumor activity of CD3-bispecific antibodies. *Sci Transl Med*. PMID: 31915305, 2020;12. doi:10.1126/scitranslmed.aaw7888.
32. Wei J, Yang Y, Wang G, Liu M. Current landscape and future directions of bispecific antibodies in cancer immunotherapy. *Front Immunol*. 2022;13:1035276. doi:10.3389/fimmu.2022.1035276. PMID: 36389699.
33. Suntharalingam G, Perry MR, Ward S, Brett SJ, Castello-Cortes A, Brunner MD, Panoskaltsis N. Cytokine storm in a phase 1 trial of the anti-CD28 monoclonal antibody TGN1412. *N Engl J Med*. 2006;355:1018–28. doi:10.1056/NEJMoa063842. PMID: 16908486.
34. Tacke M, Hanke G, Hanke T, Hünig T. CD28-mediated induction of proliferation in resting T cells in vitro and in vivo without engagement of the T cell receptor: evidence for functionally distinct forms of CD28. *Eur J Immunol*. 1997;27(1):239–47. PMID: 9022025. doi:10.1002/eji.1830270136.
35. Lühder F, Huang Y, Dennehy KM, Guntermann C, Müller I, Winkler E, Kerkau T, Ikemizu S, Davis SJ, Hanke T, et al. Topological requirements and signaling properties of T cell-activating, anti-CD28 antibody superagonists. *J Exp Med*. 2003;197(8):955–66. doi:10.1084/jem.20021024. PMID: 12707299.
36. Rodriguez-Palmero M, Hara T, Thumbs A, Hünig T. Triggering of T cell proliferation through CD28 induces GATA-3 and promotes T helper type 2 differentiation in vitro and in vivo. *Eur J Immunol*. 1999;29:3914–24. PMID: 10601999. doi:10.1002/(sici)1521-4141(199912)29:12<3914:Aid:12<3914:Aidimmu3914>3.0.Co;20. Co;2#.
37. Pallardy M, Hünig T. Primate testing of TGN1412: right target, wrong cell. *Br J Pharmacol*. 2010;161:509–11. doi:10.1111/j.1476-5381.2010.00925.x. PMID: 20880391.

38. Hanke T. Lessons from TGN1412. *Lancet*. 2006;368(9547):1569–70. author reply 1570. PMID: 17084746. doi:10.1016/S0140-6736(06)69651-7.
39. Römer PS, Berr S, Avota E, Na SY, Battaglia M, ten Berge I, Einsele H, Hünig T. Preculture of PBMCs at high cell density increases sensitivity of T-cell responses, revealing cytokine release by CD28 superagonist TGN1412. *Blood*. 2011;118:6772–82. doi:10.1182/blood-2010-12-319780. PMID: 21931118.
40. Eastwood D, Findlay L, Poole S, Bird C, Wadhwa M, Moore M, Burns C, Thorpe R, Stebbings R. Monoclonal antibody TGN1412 trial failure explained by species differences in CD28 expression on CD4+ effector memory T-cells. *Br J Pharmacol*. 2010;161:512–26. doi:10.1111/j.1476-5381.2010.00922.x. PMID: 20880392.
41. Horvath CJ, Milton MN. The TeGenero incident and the Duff Report conclusions: a series of unfortunate events or an avoidable event? *Toxicol Pathol*. 2009;37:372–83. doi:10.1177/0192623309332986. PMID: 19244218.
42. Hünig T. The storm has cleared: lessons from the CD28 superagonist TGN1412 trial. *Nat Rev Immunol*. 2012;12:317–18. doi:10.1038/nri3192. PMID: 22487653.
43. Horvath C, Andrews L, Baumann A, Black L, Blanset D, Cavagnaro J, Hastings KL, Hutto DL, MacLachlan TK, Milton M, et al. Storm forecasting: additional lessons from the CD28 superagonist TGN1412 trial. *Nat Rev Immunol*. 2012;12:740. doi:10.1038/nri3192-cl. author reply 740. PMID: 22941443.
44. Ye C, Yang H, Cheng M, Shultz LD, Greiner DL, Brehm MA, Keck JG. A rapid, sensitive, and reproducible in vivo PBMC humanized murine model for determining therapeutic-related cytokine release syndrome. *FASEB J*. 2020;34:12963–75. PMID: 32772418. doi:10.1096/fj.202001203R.
45. Peissert F, Plüss L, Giudice AM, Ongaro T, Villa A, Elsayed A, Nadal L, Dakhel Plaza S, Sciatti L, Puca E, et al. Selection of a PD-1 blocking antibody from a novel fully human phage display library. *Protein Sci*. 2022;31:e4486. PMID: 36317676. doi:10.1002/pro.4486.
46. Nagano K, Tsutsumi Y. Phage display technology as a powerful platform for antibody drug discovery. *Viruses*. 2021;13(2). PMID: 33504115. doi:10.3390/v13020178.
47. Evans EJ, Esnouf RM, Manso-Sancho R, Gilbert RJ, James JR, Yu C, Fennelly JA, Vowles C, Hanke T, Walse B, et al. Crystal structure of a soluble CD28-Fab complex. *Nat Immunol*. 2005;6:271–79. doi:10.1038/ni1170. PMID: 15696168.
48. Frank R. The SPOT-synthesis technique. Synthetic peptide arrays on membrane supports—principles and applications. *J Immunol Methods*. 2002;267(1):13–26. PMID: 12135797. doi:10.1016/S0022-1759(02)00137-0.
49. Malek TR. The biology of interleukin-2. *Annu Rev Immunol*. 2008;26:453–79. doi:10.1146/annurev.immunol.26.021607.090357. PMID: 18062768.
50. Boyman O, Sprent J. The role of interleukin-2 during homeostasis and activation of the immune system. *Nat Rev Immunol*. 2012;12:180–90. doi:10.1038/nri3156. PMID: 22343569.
51. Kaspar M, Zardi L, Neri D. Fibronectin as target for tumor therapy. *Int J Cancer*. 2006;118:1331–39. doi:10.1002/ijc.21677. PMID: 16381025.
52. Esensten JH, Helou YA, Chopra G, Weiss A, Bluestone JA. CD28 costimulation: from mechanism to therapy. *Immunity*. 2016;44:973–88. doi:10.1016/j.immuni.2016.04.020. PMID: 27192564.
53. Stebbings R, Findlay L, Edwards C, Eastwood D, Bird C, North D, Mistry Y, Dilger P, Liefvooghe E, Cludts I, et al. “Cytokine storm” in the phase I trial of monoclonal antibody TGN1412: better understanding the causes to improve preclinical testing of immunotherapeutics. *J Immunol*. 2007;179:3325–31. doi:10.4049/jimmunol.179.5.3325. PMID: 17709549.
54. Morillon YM 2nd, Sabzevari A, Schlom J, Greiner JW. The development of next-generation PBMC humanized mice for preclinical investigation of cancer immunotherapeutic agents. *Anticancer Res*. 2020;40:5329–41. PMID: 32988851. doi:10.21873/anticancer.14540.
55. Spitaleri G, Berardi R, Pierantoni C, De Pas T, Noberasco C, Libbra C, González-Iglesias R, Giovannoni L, Tasciotti A, Neri D, et al. Phase I/II study of the tumour-targeting human monoclonal antibody-cytokine fusion protein L19-TNF in patients with advanced solid tumours. *J Cancer Res Clin Oncol*. 2013;139(3):447–55. doi:10.1007/s00432-012-1327-7. PMID: 23160853.
56. Schwager K, Hemmerle T, Aebischer D, Neri D. The immunocytokine L19-IL2 eradicates cancer when used in combination with CTLA-4 blockade or with L19-TNF. *J Invest Dermatol*. 2013;133(3):751–58. PMID: 23096716. doi:10.1038/jid.2012.376.
57. Danielli R, Patuzzo R, Di Giacomo AM, Gallino G, Maurichi A, Di Florio A, Cutaia O, Lazzeri A, Fazio C, Miracco C, et al. Intralesional administration of L19-IL2/L19-TNF in stage III or stage IVM1a melanoma patients: results of a phase II study. *Cancer Immunol Immunother*. 2015;64:999–1009. doi:10.1007/s00262-015-1704-6. PMID: 25971540.
58. Millul J, Bassi G, Mock J, Elsayed A, Pellegrino C, Zana A, Dakhel Plaza S, Nadal L, Gloger A, Schmidt E, et al. An ultra-high-affinity small organic ligand of fibroblast activation protein for tumor-targeting applications. *Proc Natl Acad Sci U S A*. 2021;118(10):1073. doi:10.1073/pnas.2101852118. PMID: 3385002416.
59. Rajendra Y, Kiseljak D, Baldi L, Hacker DL, Wurm FM. A simple high-yielding process for transient gene expression in CHO cells. *J Biotechnol*. 2011;153:22–26. doi:10.1016/j.jbiotec.2011.03.001. PMID: 21392548.
60. Fairhead M, Howarth M. Site-specific biotinylation of purified proteins using BirA. *Methods Mol Biol*. 2015;1266:171–84. PMID: 25560075. doi:10.1007/978-1-4939-2272-7_12.
61. Viti F, Nilsson F, Demartis S, Huber A, Neri D. Design and use of phage display libraries for the selection of antibodies and enzymes. *Methods Enzymol*. 2000;326:480–505. PMID: 11036659. doi:10.1016/S0076-6879(00)26071-0.